

行政院國家科學委員會專題研究計畫 成果報告

低成本氣象觀測衛星之 CCD 控制邏輯及衛星星系設計

計畫類別：個別型計畫

計畫編號：NSC91-2213-E-032-007-

執行期間：91 年 08 月 01 日至 92 年 07 月 31 日

執行單位：淡江大學機械與機電工程學系

計畫主持人：洪祖昌

計畫參與人員：林宗憲,張博淵

報告類型：精簡報告

處理方式：本計畫可公開查詢

中 華 民 國 92 年 9 月 26 日

Imagery Payload Design for Passive Magnetically Stabilized Microsatellite

Abstract

The charge-coupled device (CCD) control logic design and analysis of pointing knowledge of a low-cost microsatellite, the Taiwan Universities United satellite (TUUSAT), which applies passive magnetic attitude control system is discussed. The CCD mission of TUUSAT requires transmitting at least one image covering Taiwan, Republic of China, per day. To meet the mission requirements, a shooting zone centered at Taiwan is determined according to the regression of orbit and the spin rate of the satellite. Two cameras are employed in the present design. A simple scheme of CCD control logic is provided to determine the proper timing of shooting images. The determination of optimal setup angle of cameras in the satellite with the minimal pointing errors is analyzed. The simulation result shows the CCD control logic design and the selection of setup angle of cameras satisfactorily met the CCD mission requirement. It is found that the control system design for the specified CCD mission can also be applied to the other places located at the same geomagnetic latitude as that of Taiwan.

低成本氣象觀測衛星之 CCD 控制邏輯及衛星星系設計

本文為低成本氣象衛星 TUUSAT(Taiwan Universities United satellite)的 CCD(電荷耦合元件)控制邏輯設計和分析，姿態的控制是運用被動式控制系統。CCD 的任務為每天傳送最少一張覆蓋台灣的氣象雲圖。為了符合此需求，要依據衛星軌道的退行率和自旋率去算出照相的中心點。此設計是運用兩台 CCD 去達成任務，提供一個 CCD 控制邏輯的簡單系統，去算出照相的合適時間，衛星上 CCD 的最佳安裝角度是由最小指向錯誤分析而得到。其模擬的結果顯示 CCD 控制邏輯設計和相機安裝角度的選擇能滿足此 CCD 的任務需求。CCD 控制邏輯也顯示在流程圖中，我們也發現此 CCD 任務控制系統的設計也可運用在和台灣同一緯度的其他地方上。

Keyword: Mission Design, Imagery Payload, Attitude control

Introduction

Recently, more space mission research implemented in universities is focused on the development of micro- or nanosatellites that are designed as a secondary payload of most space vehicles. These satellites possess the same features of being low-cost, simple, fast to build and able to operate in low earth orbit (LEO). In order to achieve these features, researchers attempt to build spacecraft that comprise simple and low-cost subsystems using off-the-shelf components. For example, several micro- and nanosatellite programs in universities attempted to apply a passive attitude control system that comprised magnetic rods and hysteresis dampers.

In 1990, Webersat (WO-18)¹ applied a passive magnetic attitude control system and CCD on a satellite. The CCD payload of WO-18 was setup on the lateral sides of satellite for Earth images. However, there was no control logic design for the CCD and each Earth image obtained from the camera was not predetermined. Actually, there are no predetermined shooting targets for their CCD strategy. Similar satellites, SAPPHIRE² and Spartnik³, also have passive control systems, and CCD payloads were mounted on the top of the satellite. The CCD missions of SAPPHIRE and Spartnik are to obtain pictures of North America. A simple CCD operation strategy is employed to fit the CCD mission requirement. When the satellite passes over the higher latitudes of the northern hemisphere, the CCD has good pointing to the nadir due to the small angle between the direction of geomagnetic field and the ground vertical, as shown in Fig. 1. In 1999, the similar system and CCD operation strategy was applied to the nanosatellite MUNIN⁴. A miniature CCD was setup on the lateral side of satellite. The objective for MUNIN satellite was to collect data on the auroral activity in both the northern and southern hemispheres. However, the simple CCD operation strategy only fits at higher latitudes and the details of pointing error were not discussed. The limitation of the latitude in which the camera could have good pointing to the nadir for good Earth images was not clear.

In this paper, a similar passive control system and CCD are implemented on Taiwan Universities United Satellite (TUUSAT).⁵ Different from the former simple CCD strategy of SAPPHIRE, Spartnik and MUNIN, the CCD mission of TUUSAT is to shoot weather images above Taiwan, Republic of China (121.13 deg E, 23.97 deg N), located at low latitude near the equator. Taiwan is also located in the cyclone tropic and many typhoons pass through every year, primarily from July to November. The weather images are valuable for meteorologists to observe and predict the dynamic trends of typhoons.

The missions of TUUSAT are to obtain CCD Earth images, global positioning system (GPS), and communication experiments, and voices broadcasting. It was assumed to have a sun-synchronous orbit with 98.6 deg inclination and 800 km height. The main structure and main feature of the bus system is quite similar to that of SAPPHIRE, Spartnik and MUNIN. A detailed description of TUUSAT bus will not be discussed here. The hardware of the passive attitude control system is also very similar to SAPPHIRE, Spartnik and MUNIN. The main work of this paper concerns design and implementation of the control logic for the CCD mission requirements which we assumed that the CCD will be able to transmit one weather image file per day of the area over Taiwan.

Attitude control system

Passive magnetic attitude control system has been applied to several satellites

successfully, such as Vanguard satellite (1958), TRANSIT satellites (1960), and early OSCAR series satellites, among others. This kind of attitude control system comprises strong permanent magnetic rods and well-designed hysteresis dampers, such as hysteresis rods and shorted coils. The stability and behavior of spacecraft motion were studied by Fischell, Kammuler and Chen⁶⁻⁹. Fischell⁶ discussed the spin removal by means of eddy current damping and shorted coil damping. The despin rate of the satellite was also calculated⁷ and generally agreed with the observed data of TRANSIT satellites. Kammuler⁸ investigated the roll resonance solution of magnetically stabilized satellite and used a variational approach and the Ritz numerical method. The policy for selection of inertial parameters was defined to optimize the stable region. Chen⁹ developed the dynamic equation of passive magnetically oriented satellite. Two types of damping scheme (hysteresis rods and shorted coils) were studied separately.

As shown in Fig. 2, the attitude control system of TUUSAT contains four permanent magnetic rods coinciding with the satellite's spin axis (z-axis) and one set of shorted coils perpendicular to z-axis. The attitude of satellite is determined by employing the magnetometer and sun sensor which utilized the solar panels. The simulation of dynamic equations, including magnetic restoring and damping torques similar to Chen⁹, has been done for TUUSAT's attitude control system in Ref. 5 and 10. The results showed that the satellite will spin with 0.05 to 0.1 rpm after about 30 orbits and that the maximal misalignment from the z-axis to the local field direction is about 10 deg. The relation between z-axis and local field direction can be given by

$$\mathbf{z} \bullet \mathbf{b} = \cos \Omega \quad ; \quad \Omega \leq 10 \text{deg} \quad (1)$$

The simulation of attitude motion of TUUSAT in Ref. 5 and 10 have a good agreement with that of Chen's⁹ results. The result will be adopted in this paper for the CCD control logic design and analysis of pointing knowledge.

Mission analysis

CCD payload and mission requirements

The CCD payload of TUUSAT contains two cameras, which are setup each on the opposite side of the lateral of satellite with setup angle S as shown in Fig. 3. The reason of employing two cameras will be shown later. The relations between the directions of cameras and \mathbf{z} can be expressed as

$$\mathbf{c} \bullet \mathbf{z} = \cos S \quad (2)$$

where \mathbf{c} lies on the y-z plane in Fig. 3. Here, \mathbf{c} is defined as one of the two cameras' directions, which point to the ground. A distinguishing equation is given by the following. For $n = 1, 2$, if there exists

$$\mathbf{c}_n \bullet \mathbf{r} \leq 0, \text{ then } \mathbf{c} = \mathbf{c}_n. \quad (3)$$

The CCD is an electrical camera with wide angle (about 100 deg) and the

memory size of each image file is less than 200 KB. The image coverage is about 2127km x 2127km when the CCD vertically points to the nadir, as shown in Fig. 4. The camera is estimated to transmit one image file per day due to the limited transmit rate of the transceiver. As shown in Fig. 1, the relation¹ between \mathcal{U} and θ_{m2} can be expressed as

$$\mathcal{U} = 90 - \tan^{-1}(2 \tan \theta_{m2}) \quad (4).$$

Because the angle θ_{m2} of Taiwan is 13.7, the angle \mathcal{U} over Taiwan calculated from Eq. (4) is 64. To achieve the proper pointing of the CCD, the CCD must be setup on the lateral side of satellite due to the large angle \mathcal{U} of Taiwan.

The mission requirements of TUUSAT's CCD payload are described as follows. First, the images must cover Taiwan or Taiwan must be within the field of view (FOV) of the CCD. Second, since the transmit rate of the communication subsystem is not fast, it requires shooting and transmitting one image file per day. Third, the CCD control logic is implemented in the flight software.

Pointing knowledge

Because the satellite spins about z-axis and the cameras are setup on the lateral sides, the directions of cameras will rotate about the z-axis. When the satellite passes over at a lower latitude, the FOV of camera will sweep the ground surface with a wide angle ($\mathcal{L}=100$ deg) as shown in Fig. 5. The camera can shoot images covering Taiwan when the camera's FOV sweeps to cover Taiwan. It is evident that the pointing direction of the camera always changes, thus the pointing of camera cannot be kept at a fixed direction. The pointing error is defined as the angle between the camera's direction and the position vector from the satellite to the shooting target, and is given by

$$\Phi = \cos^{-1}(\mathbf{c} \cdot \mathbf{l}) \quad (5).$$

The pointing knowledge, which guarantees the images will cover Taiwan, is then denoted as the maximum allowable pointing error which is equal to half of \mathcal{L} .

Because the magnetic rods are setup on the z-axis of satellite, the direction of \mathbf{z} can be considered as related to the local field direction. For convenience of our analysis, denote \mathbf{z}_o as the reference direction of the z-axis under the assumption which \mathbf{z} exactly coincides with \mathbf{b} or $\Omega=0$ in Eq. (1). Therefore, \mathbf{z}_o can be obtained at any location in orbit from the mathematical model of geomagnetic field. To correspond to \mathbf{z}_o , here \mathbf{c}_o is denoted as reference vector of the CCD that can be determined by substituting \mathbf{c}_o and \mathbf{z}_o into Eqs. (2) and (3). The reference pointing error Φ_o is then defined as

$$\Phi_o = \cos^{-1}(\mathbf{c}_o \cdot \mathbf{l}) \quad (6).$$

Because the z-axis oscillates about the local field direction, the direction of the z-axis usually does not coincide with the local field direction. As shown in Fig. 6, \mathbf{z}

oscillates about \mathbf{b} within 10 deg, and the misalignment from \mathbf{z} to \mathbf{b} is Ω . Here \mathbf{c} and \vec{c}_o lie on the y-z plane and the angle between \vec{c} and \vec{c}_o is $\Delta\Phi$. The relation between \vec{c} and \mathbf{c}_o can be expressed as

$$\mathbf{c} \bullet \mathbf{c}_o = \cos \Delta\Phi, \quad 0 \leq \Delta\Phi \leq \Omega \leq 10 \text{ deg} \quad (7)$$

Equation (7) shows the misalignment of the camera's pointing caused by oscillating motion of satellite. The relation of Φ and Φ_o can be written as $\Phi_o - \Delta\Phi \leq \Phi \leq \Phi_o + \Delta\Phi$ (8).

The range of pointing error can also be given as $\Phi_o - \Omega \leq \Phi \leq \Phi_o + \Omega$ (9).

To meet the requirement of pointing knowledge, the pointing error should satisfy

$\Phi \leq \frac{\mathcal{F}}{2}$. Hence, the reference pointing error should satisfy

$$\Phi_o \leq \frac{\mathcal{F}}{2} + \Omega \leq 40 \quad (10).$$

Equation (10) shows the range of reference pointing error which guarantees the image will cover Taiwan. To meet Eq. (10), the design of CCD control logic will be given later.

Shooting Zone

Because the mission requires transmitting one image per day, we defined an area including Taiwan that is denoted as the shooting zone. The shooting zone is chosen such that the satellite should pass over it every day. During this pass, one might have chance to shoot the images covering Taiwan.

Because the orbit is sun synchronous, the satellite will pass over the local horizon of shooting target two or three times per day with different footprints as shown in Fig. 7. The numbers 1 to 5 represent the first to fifth ascending node. The regression of ascending nodes per revolution of orbit is denoted as L_r at equator. The distances of L_r between each node are all equal. This means the satellite will pass through each interval of L_r at least one time per day. If the configuration of shooting zone is a rectangle and the width of shooting zone is L_r , the satellite will pass over the shooting zone every day. The regression of nodes¹¹ is expressed as

$$L_r = (\mathcal{S}_e - \dot{\Theta})P \quad (11)$$

where $\dot{\Theta} = -2.3963 \times 10^9 \frac{\cos i}{a^{3.5}(1-e^2)^2}$.

Because two cameras are setup on the lateral sides of satellite, the directions of cameras will rotate about z-axis around 360 deg as the satellite spins half of a revolution. This guarantees that there is at least one camera pointing to ground as the

satellite spins per half-revolution. When the satellite spins half of a revolution, the footprint of satellite will move a length of distance. Hence, at least one camera will point to ground at this length of distance. The ground track¹¹ of satellite when it spins over the time t_s can be calculated as follows,

$$La = \sin^{-1}(\sin i \sin A_{la})$$

$$l_o = \sin^{-1}\left(\frac{\tan La}{\tan i}\right) \quad (12).$$

$$L_o = -l_o + \dot{\Theta} t_s - \tilde{S}_e t_s$$

As shown in Fig. 8, the shooting zone **D** is a rectangle area centered at Taiwan with width l_w and height l_h , where **H** is the local horizon of Taiwan; l_w and l_h can be determined by following two equations:

$$l_w = -L_r - L_o \quad (13)$$

$$l_h = La \quad (14)$$

Because the lowest spin rate of satellite is 0.05 rpm, the longest spin time t_s for a half-revolution is 10 minutes. For the orbit of TUUSAT, $i=98.6$, $a=7178$, and $e=0$, the width and height of shooting zone are $l_w=33.9$ and $l_h=35.2$, respectively. The range of shooting zone is inside the range of **H**. If only one camera setup on the satellite is used, the camera will point to ground as the satellite spins one revolution. The longest spin time t_s for one revolution is 20 min. Then l_w and l_h become 39.7 and 70.44, respectively, and the shooting zone will be out of the range of **H**. To guarantee the satellite is inside the range of **H** when the camera points to ground in **D**, at least two cameras are needed. In the present analysis, two cameras are employed.

The shooting zone, **D**, can be represented as $\mathbf{D} = \mathbf{D} (s_1, s_2)$ (15)

where $G_{lo} - \frac{l_w}{2} \leq s_1 \leq G_{lo} + \frac{l_w}{2}$, $G_{la} - \frac{l_h}{2} \leq s_2 \leq G_{la} + \frac{l_h}{2}$,

and $G_{la} = 24.97^\circ N$, $G_{lo} = 121.13^\circ E$, $l_w = 33.9$, $l_h = 35.2$.

In this shooting zone, it guaranteed the satellite will pass over and one of the cameras will point to ground at least one time per day. Then we can shoot and transmit at least one ground image of the shooting zone per day. However, the images may not cover Taiwan without a proper CCD control logic design. To ensure that the images cover Taiwan, a well-designed CCD control logic should be investigated.

Design of CCD control logic

Logic Design

To ensure that the images cover Taiwan, it is necessary to analyze the variation of the camera's direction, which is related to local geomagnetic field. As shown in Fig.

9, the geomagnetic field¹² is expressed as dipole model and given by

$$\mathbf{B} = \frac{\tilde{E}}{r^3} (-2 \sin \theta_m \mathbf{e}_r + \cos \theta_m \mathbf{e}_\theta) \quad (16)$$

where $\mathbf{e}_\theta = \mathbf{e}_r \times \mathbf{e}_\phi$.

Define $\mathbf{Fg} (\mathbf{X}, \mathbf{Y}, \mathbf{Z})$, $\mathbf{Fm} (\mathbf{x}_m, \mathbf{y}_m, \mathbf{z}_m)$ and $\mathbf{Fs} (\mathbf{e}_n, \mathbf{e}_r, \mathbf{e}_\theta)$ as geographic frame, geomagnetic frame, and spherical frame, respectively. The transformations between each frame are expressed as

$$\begin{bmatrix} \mathbf{e}_n \\ \mathbf{e}_r \\ \mathbf{e}_\theta \end{bmatrix} = \begin{bmatrix} c_{\theta_m} c_{\theta_n} & s_{\theta_m} c_{\theta_n} & s_{\theta_m} \\ -s_{\theta_m} & c_{\theta_m} & 0 \\ -c_{\theta_m} s_{\theta_n} & -s_{\theta_m} s_{\theta_n} & c_{\theta_m} \end{bmatrix} \begin{bmatrix} \mathbf{x}_m \\ \mathbf{y}_m \\ \mathbf{z}_m \end{bmatrix} \quad (17)$$

$$\begin{bmatrix} \mathbf{x}_m \\ \mathbf{y}_m \\ \mathbf{z}_m \end{bmatrix} = \begin{bmatrix} c\theta_1 & s\theta_1 & 0 \\ -s\theta_1 c\theta_2 & c\theta_1 c\theta_2 & s\theta_2 \\ s\theta_1 s\theta_2 & -c\theta_1 s\theta_2 & c\theta_2 \end{bmatrix} \begin{bmatrix} \mathbf{X} \\ \mathbf{Y} \\ \mathbf{Z} \end{bmatrix} \quad (18)$$

where s and c denote trigonometric sin and cos functions. As shown in Fig. 10, the angles θ_1 and θ_2 represent the angle between \mathbf{X} and \mathbf{x}_m , and the inclination between geographic and geomagnetic North Pole, respectively. The angle θ_m and θ_n in \mathbf{Fm} can also be transferred to θ_1 and θ_2 in \mathbf{Fg} from Eqs. (17) and (18).

Equation (16) can be represented in \mathbf{Fm} as unit vector as,

$$\mathbf{b} = \frac{\mathbf{B}}{|\mathbf{B}|} \quad (19)$$

where

$$\mathbf{B} = \frac{\tilde{E}}{r^3} [(2 s_{\theta_m} s_{\theta_n} - c_{\theta_m} c_{\theta_n} s_{\theta_m}) \mathbf{x}_m + (-2 c_{\theta_m} s_{\theta_n} - s_{\theta_m} s_{\theta_n} c_{\theta_m}) \mathbf{y}_m + (-2 c_{\theta_m} s_{\theta_n} + c_{\theta_m}^2 s_{\theta_n}) \mathbf{z}_m]$$

As shown in Fig. 11, the vector \vec{l} is expressed as

$$\mathbf{l} = \frac{\mathbf{g} - \mathbf{r}}{|\mathbf{g} - \mathbf{r}|} \quad (20)$$

where

$$\mathbf{g} = \text{Re} [(cG_{lo} cG_{la} c\theta_1 + (cG_{lo} cG_{la} s\theta_1 s\theta_2 - s$$

$$(21)$$

and

$$\mathbf{r} = \dots [(c_{\theta_1} c_{\theta_2} c\theta_1 + s_{\theta_1} - s_{\theta_1} c_{\theta_2} c\theta_1 s\theta_2 + s_{\theta_2} c$$

$$(22)$$

To determine the proper timing of shooting the image to meet the requirement of

pointing knowledge, a simple scheme of CCD control logic is given by

$$\mathbf{c} \bullet (\mathbf{l} \times \mathbf{b}) = 0 \quad (23)$$

In Eq. (23), \mathbf{l} and \mathbf{b} comprise the plane which includes the shooting target and is denoted as \mathcal{S} , the cross-hatched plane shown in Fig. 11. When the satellite passes over \mathbf{D} , then \mathbf{l} and \mathbf{b} will compose \mathcal{S} , and the direction of cameras will rotate about the spin axis such that \mathbf{c} will lie on \mathcal{S} somewhere over \mathbf{D} . When the direction of CCD lies on \mathcal{S} , it is obvious the pointing error Φ is only related to setup angle \mathcal{S} . Therefore, a proper choice of \mathcal{S} could minimize the pointing error.

Analysis of pointing knowledge

Assume there are $j \times k$ ($j=34$, $k=36$) sample points with equal spacing over \mathbf{D} where j and k are along the direction of l_w and l_h , respectively. Each sample points meets the requirement Eq. (23). Then, one set of reference pointing errors at these points can be obtained according to Eq. (6). For the present analysis, the root mean square and maximal value of the Φ_o functions of \mathcal{S} are given as follows:

$$\Phi_{oM}(\mathcal{S}) = \sqrt{\frac{\sum_{j=1}^j \sum_{k=1}^k \Phi_{o,j,k}^2(\mathcal{S})}{j \times k}} \quad (24)$$

$$\Phi_{o\max}(\mathcal{S}) = \max(\Phi_{o,j,k}(\mathcal{S})) \quad (25)$$

where $j=1,2,\dots,34$, $k=1,2,\dots,36$, which represents the j^{th} and k^{th} sample point along l_w and l_h , respectively, and $0 \leq \mathcal{S} \leq 180$. The value of \mathcal{S} was considered as a parameter to be given once at each time of calculation to obtain the values of Φ_{oM} and $\Phi_{o\max}$ according to Eqs. (24) and (25).

The distributions of Φ_{oM} and $\Phi_{o\max}$ vs. \mathcal{S} are calculated and shown in Fig. 12. Fig. 12 shows that $\Phi_{o\max} \leq 40$ occurs when $62 \leq \mathcal{S} \leq 70$, and the minimum $\Phi_{o\max} = 35$ occurs when $\mathcal{S} = 66$. If the setup angle was selected in the range of 62-70 deg, $\Phi_{o\max}$ will be less than 40, which meets the reference pointing knowledge of Eq. (10). Fig.12 also shows that the optimal setup angle \mathcal{S}_{opt} is 66 which is minimum value of $\Phi_{o\max}$.

For $\mathcal{S} = 66$, the distribution of Φ_o in \mathbf{D} is shown in Fig. 13. Here, Φ_{oM} is 23 and $\Phi_{o\max}$ is 35. When $\Phi_{oM} = 23$ is substituted into Eq. (9), the range of mean pointing error is $13 \leq \Phi_M \leq 33$. Thus, the optimal setup angle of 66 deg also provides the minimum pointing errors. These results satisfy the CCD mission requirement well.

Implementation of CCD control logic

The implementation of CCD control logic is shown as the flowchart in Fig. 14. Each steps in Fig. 14 is described as follows.

- 1) Input the data such as the location of shooting target G_{lo} and G_{la} , the setup

angle \mathcal{S} , the size of shooting zone \mathcal{I}_w and \mathcal{I}_h , and establish the range of the shooting zone in the flight software, according to Eq. (15).

2) Receive the data of \mathcal{M}_1 and \mathcal{M}_2 from GPS. Estimate if the satellite is inside the shooting zone by Eq. (15).

3) Calculate the unit vectors of \mathbf{l} , \mathbf{c} , and \mathbf{b} according to the information provided by the onboard sensors. The position vector \mathbf{l} can be obtained by substituting \mathcal{M}_1 and \mathcal{M}_2 into Eqs. (20-22). The attitude of the three axes of the satellite can be obtained from an attitude sensor, such as a magnetometer. Then \mathbf{c} can be obtained from Eqs. (2) and (3), and \mathbf{b} can be calculated from the geomagnetic field model in the flight software.

4) Substitute \mathbf{l} , \mathbf{c} , and \mathbf{b} into Eq. (23). Determine if Eq. (23) is satisfied.

5) Shoot images and store them in the onboard computer. Send message back to ground station and inform the picture has been taken.

Extended application for other shooting targets

The present CCD mission design can also be applied to take weather images other than above Taiwan if the targets were located at the same geomagnetic latitude as that of Taiwan. Detail of this analysis is given next.

In Eq. (4), the angle \mathcal{U} from the local field direction to the local ground vertical is a function of geomagnetic latitude \mathcal{M}_2 . If the selected shooting targets are located at the same geomagnetic latitude as Taiwan, this can be expressed as

$$\mathbf{G}_{m1} = (G_{lo}(\mathcal{M}_1, \mathcal{M}_2), G_{la}(\mathcal{M}_1, \mathcal{M}_2)), \quad 0 \leq \mathcal{M}_1 \leq 360, \quad \mathcal{M}_2 = 13.96 \quad (26).$$

When Eq. (26) is substituted into Eq. (15), one set of shooting zones can be obtained along \mathbf{G}_{m1} . Then \mathcal{S}_{opt} , $\Phi_{o\max}$, and Φ_{oM} of each shooting zone can be obtained

from Eq. (24) and (25). The distributions of \mathcal{S}_{opt} , $\Phi_{o\max}$, and Φ_{oM} along \mathbf{G}_{m1} are

shown in Fig. 15. Fig. 15 shows that \mathcal{S}_{opt} , $\Phi_{o\max}$, and Φ_{oM} are almost the same as Taiwan at different geomagnetic longitude. This means that the present design of the CCD payload mission fits other targets that are located at the same geomagnetic latitude as Taiwan.

If the selected shooting targets were located at the same geomagnetic longitude as but different geomagnetic latitude from that of Taiwan, the shooting targets can be expressed as

$$\mathbf{G}_{m2} = (G_{lo}(\mathcal{M}_1, \mathcal{M}_2), G_{la}(\mathcal{M}_1, \mathcal{M}_2)), \quad \mathcal{M}_1 = 100.84, \quad 0 \leq \mathcal{M}_2 \leq 90 \quad (27).$$

When Eq. (24) is substituted into Eq. (15), one set of shooting zones can be obtained along \mathbf{G}_{m2} . The distributions of \mathcal{S}_{opt} , $\Phi_{o\max}$, and Φ_{oM} along \mathbf{G}_{m2} are shown in Fig.

16. Fig. 16 shows that S_{opt} at the geomagnetic equator and geomagnetic North Pole are 90 and 18, respectively. S_{opt} varies from 90 to 26 when θ_{m2} of the shooting target changes from 0 to 90. When the shooting target is selected at different geomagnetic latitudes, the optimal setup angle of CCD cannot be fixed. In this case, a movable camera with changing S in the satellite is then needed. This remains for further study.

As a demonstration, the following places are selected to apply the present CCD mission design. For example, we can use the same setup angle for TUUSAT to shoot the targets that lie on G_{m1} and located in Sudan, the People's Republic of China or Colombia. Those places are located at 32.4785 ° E, 16.5761 ° N, 108.8 km N of Khartoum, Sudan, and 113.7942 ° E, 25.1588 ° N, 227.7 km SE of Hengyang, People's Republic of China, and 90.4 ° W, 2.2158 ° N, 276.4 km SSE of Bogota, Colombia, respectively. The distributions of reference pointing errors in those targets are shown in Figs. 17-19. These results show that the reference pointing errors satisfy the reference pointing knowledge of Eq. (10), which guarantees the images will cover the shooting targets.

Conclusions

Application of a passive magnetically oriented satellite to take weather images of lower latitude is extended. A CCD payload with implemented control logic design was proposed to meet the mission requirement of transmitting at least one image of Taiwan per day. The selection of the shooting zone, the optimal selection of the setup angle of the cameras in satellite, and the minimum pointing errors were presented. For the same mission requirement, it also found that the application of the present design could be extended to areas that possess the same geomagnetic latitude as that of Taiwan.

Reference

- ¹White, J., "Microsat Motion, Stabilization, and Telemetry," Radio Amateur Satellite Corporation-North America Journal, Vol. 13, No. 4, Nov. 1990, pp. 13-30.
- ²Lu, R. A., "Building 'Small, Cheaper, Faster' Satellites within the Constraint of an Academic Environment," the 9th Annual AIAA/USU Conference on Small Satellites, Logan, Utah, Sept. 1995.
- ³Menges, B. M., Guadamos, C. A., and Lewis, E. K., "Dynamic Modeling of Micro-Satellite Spartnik's Attitude," Region VI AIAA Student Conference, Seattle, Washington, April 1997.
- ⁴Ovchinnikov, M., Pen'kov, V., "Attitude Control System for The First Swedish Nanosatellite MUNIN," Acta Astronautica, Vol. 46, Nos. 2-6, 2000, pp. 319-326.

⁵Hong, Z. C., "The System Engineering Analysis and System Conceptual, Preliminary and Detailed Designs of Micro-Satellite," NSC-87-2612-E-008-006, Final Report of National Science Council, Taipei, Taiwan, 1995~1998.

⁶Fischell, R. E., "Magnetic Damping of the Angular Motion of Earth Satellite," America Rocket Society Journal, Vol.31, No. 9, Sept. 1961, pp. 1210-1217.

⁷Fischell, R. E., "Passive Magnetic Attitude Control for Earth Satellite," Advances in Astronautical Sciences, Vol. 11, Jan. 1962, pp. 147-177.

⁸Kammuler, R. W., "Roll Resonance and Passive Roll Control of Magnetically Stabilized Satellite," AIAA Journal, Vol. 10, No. 2, 1972, pp. 129-136.

⁹Chen, Y., "The Damped Angular Motion of a Magnetically Oriented Satellite," Journal of The Franklin Institute, Vol. 280, No. 4, 1965, pp. 291-306.

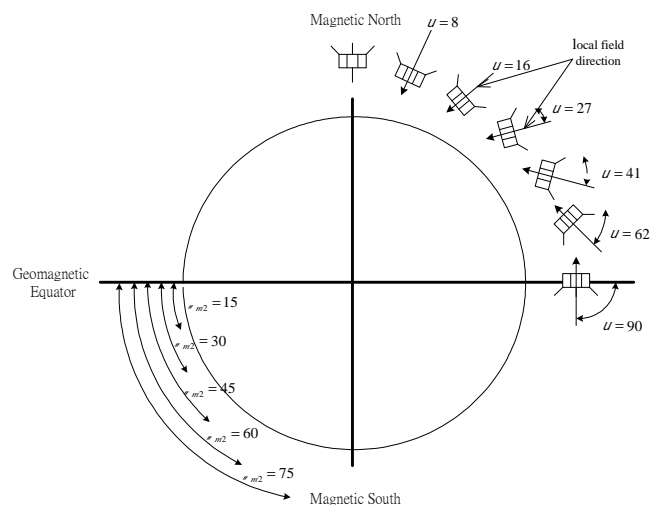
¹⁰Lin, C. H., Shih, C. H., Chuang, C. K., "The Passive Magnetic Stabilization used

Magnetic Rods for a Microsatellite TUU SAT-1," 50th International Astronautical Congress, Amsterdam, The Netherlands, IAF-ST-99 -W.1.06, Oct. 1999.

¹¹Brown, C. D., "Spacecraft Mission Design," AIAA, Washington, DC, 1992, pp. 55-79.

¹²Chobotov, V. A., "Spacecraft Attitude Dynamics and Control," Krieger Publishing Company, Florida, 1991, pp. 77-90.

本報告內容已發表於 **AIAA Journal Spacecraft and Rockets, Vol. 40, No. 3, May-June 2003.**



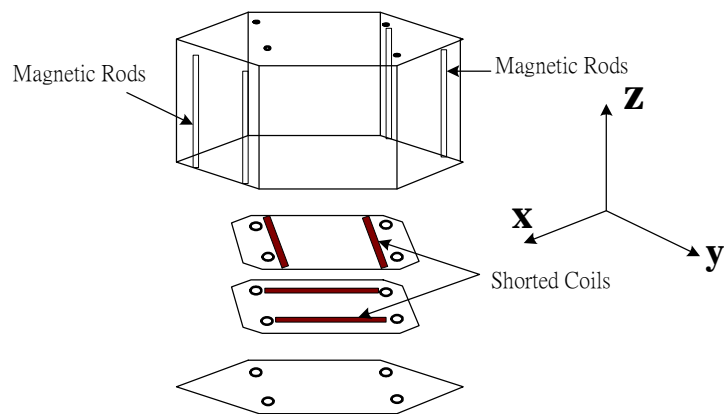


Fig.1 The angle between local field direction and local horizon

Fig. 2 The configuration of TUUSAT

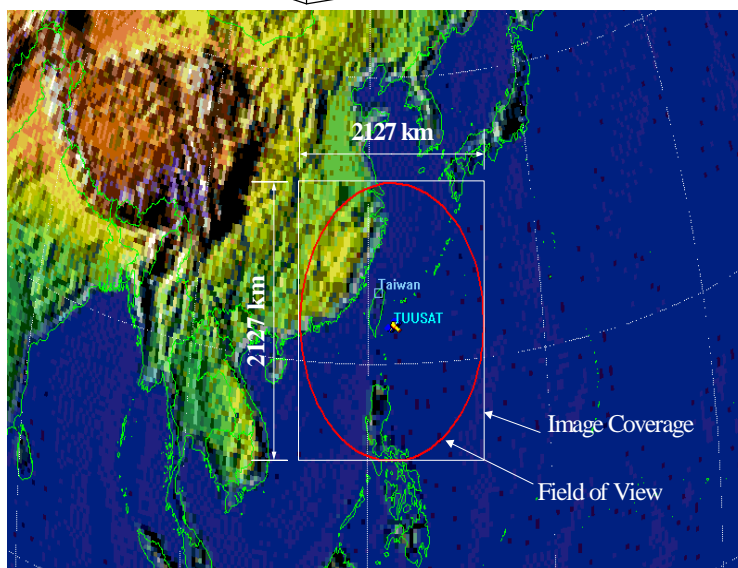
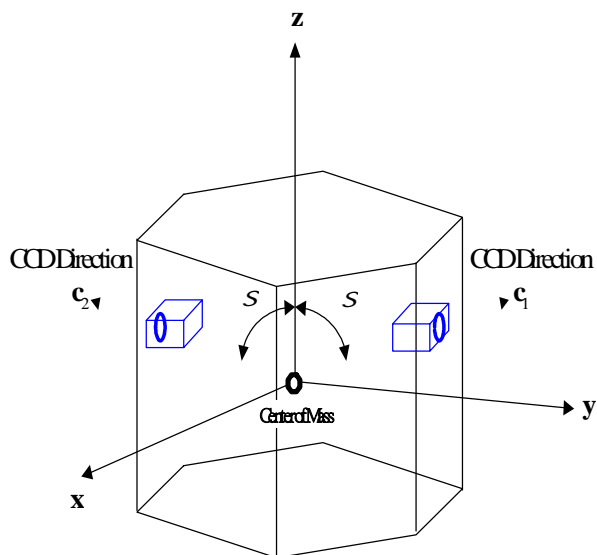


Fig. 3 Contribution of TUUSAT's CCD payload

Fig. 4 Image coverage of

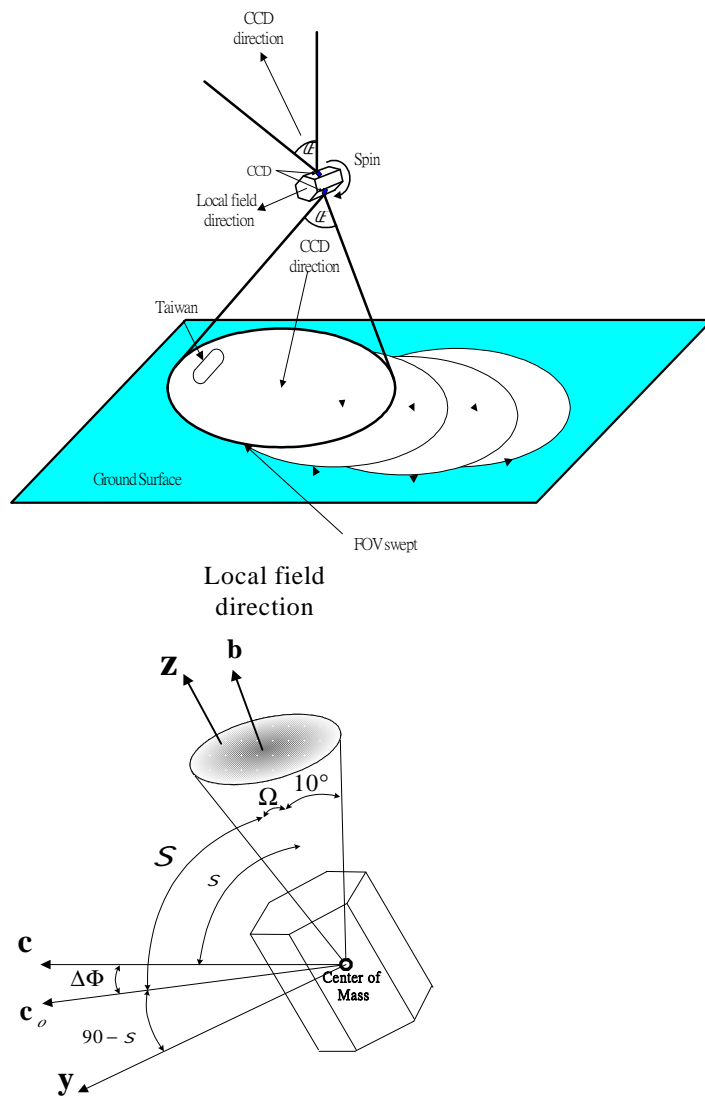
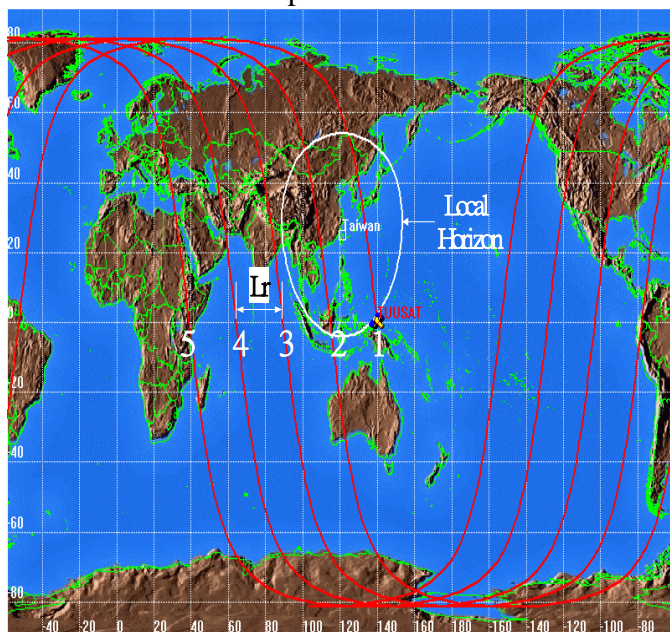


Fig. 5 The camera sweeps the ground surface caused by oscillation as the satellite spins

Fig. 6 The pointing error



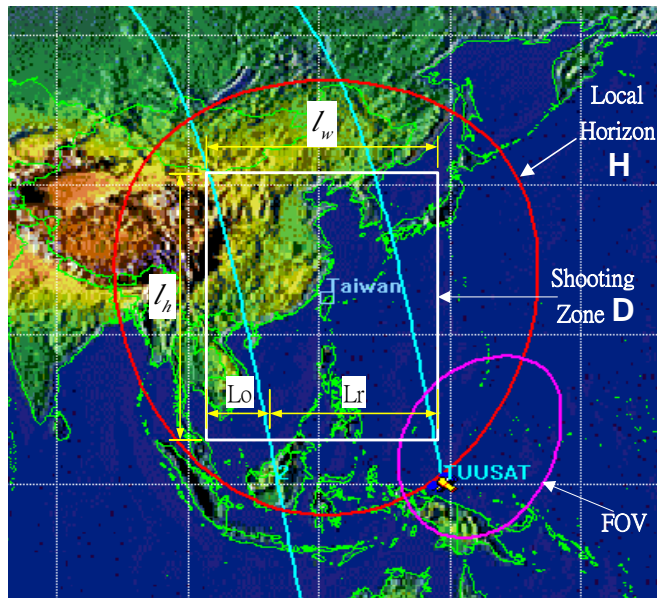
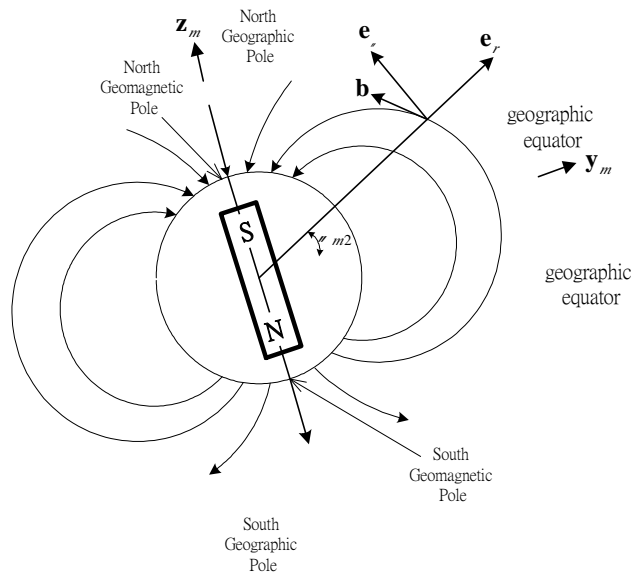


Fig. 7 The orbital tracking of TUUSAT of TUUSAT

Fig. 8 The shooting zone



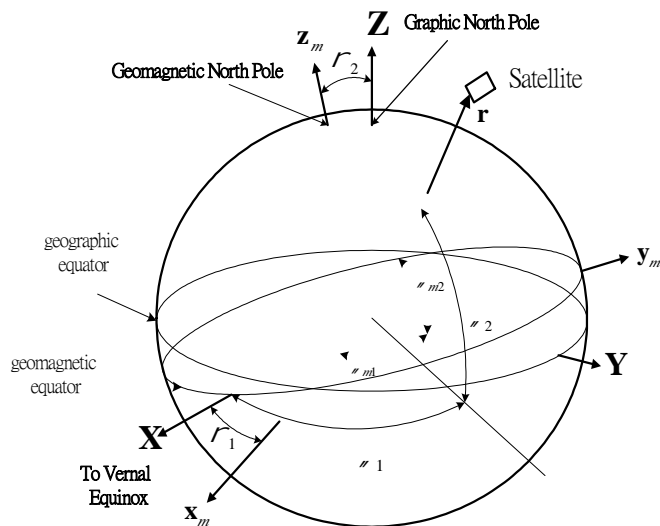


Fig. 9 Geomagnetic field dipole model

Fig. 10 The geometric frame $\mathbf{F}_g(X, Y, Z)$ and geomagnetic frame $\mathbf{F}_m(x_m, y_m, z_m)$

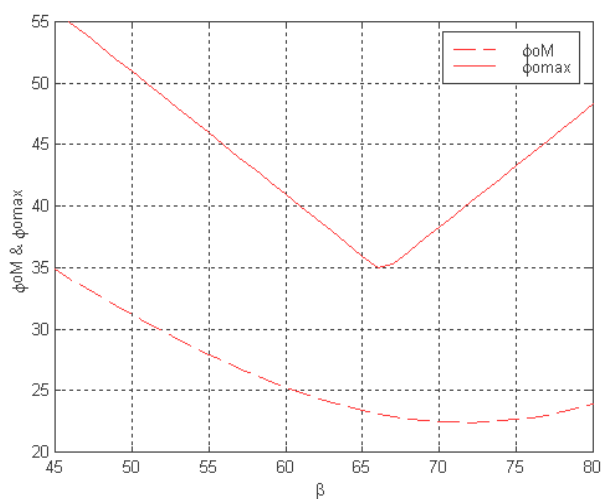
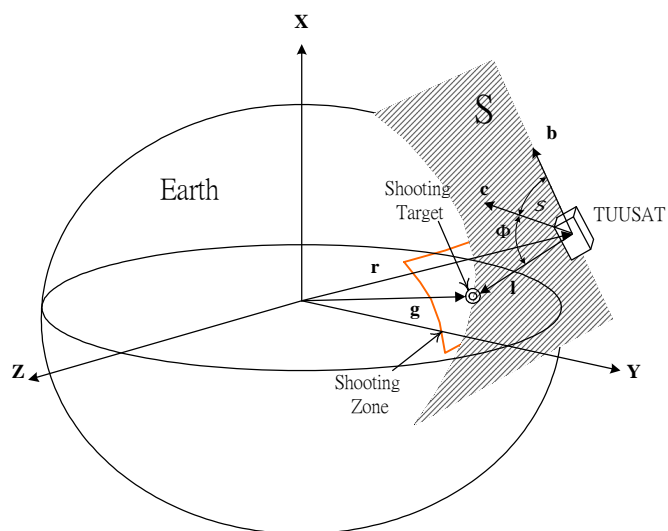


Fig.11 The geometry of the CCD direction and satellite Fig.12 The distributions

of $\Phi_{o\max}$ and Φ_{oM} vs. S

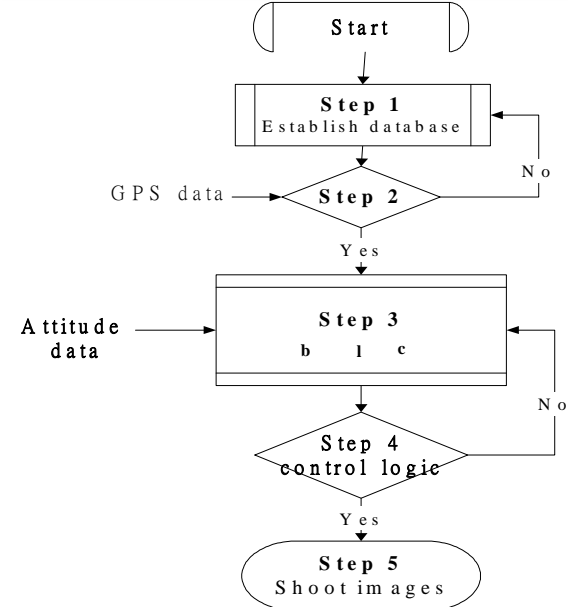
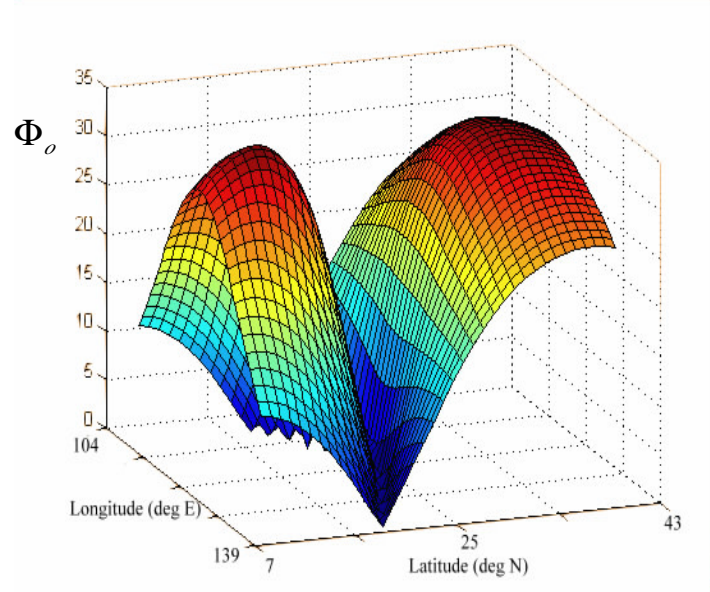


Fig. 13 The reference pointing error Φ_o of Taiwan in **D**

Fig. 14 The flowchart of the implementation of CCD control logic

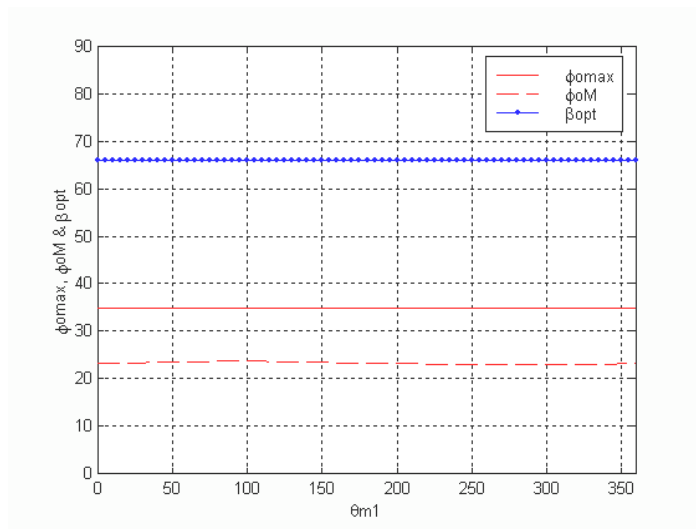


Fig. 15 S_{opt} , Φ_{oM} and Φ_{omax} along G_{m1}

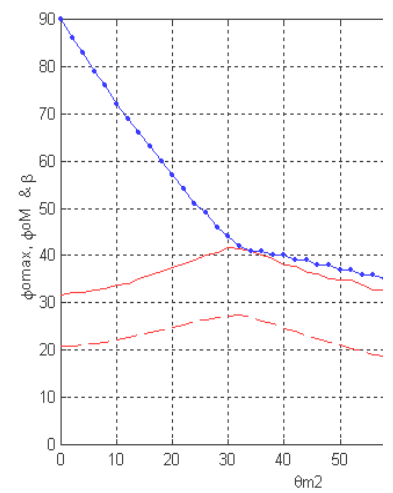
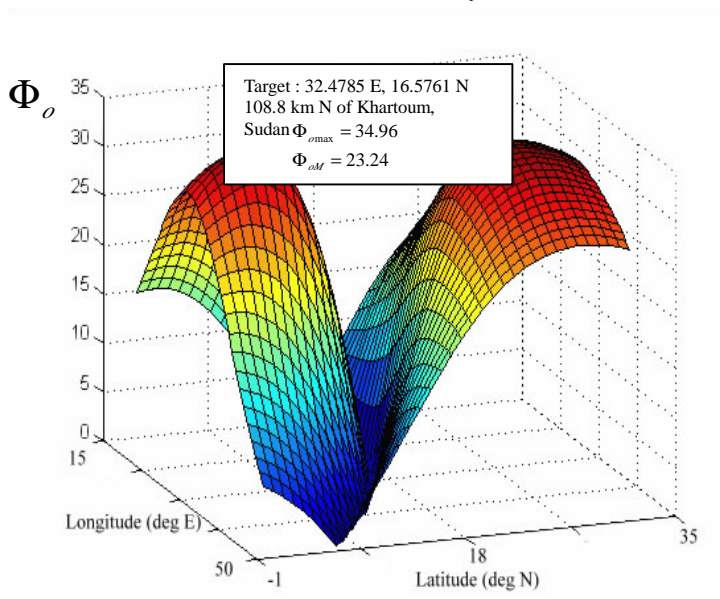


Fig. 16

Parameters S_{opt} , Φ_{oM} and Φ_{omax} along G_{m2}



Φ_o

Target : 113.7942 E, 25.1588 N
227.7 km SE of Hengyang, China
 $\Phi_{omax} = 34.95$
 $\Phi_{oM} = 23.66$

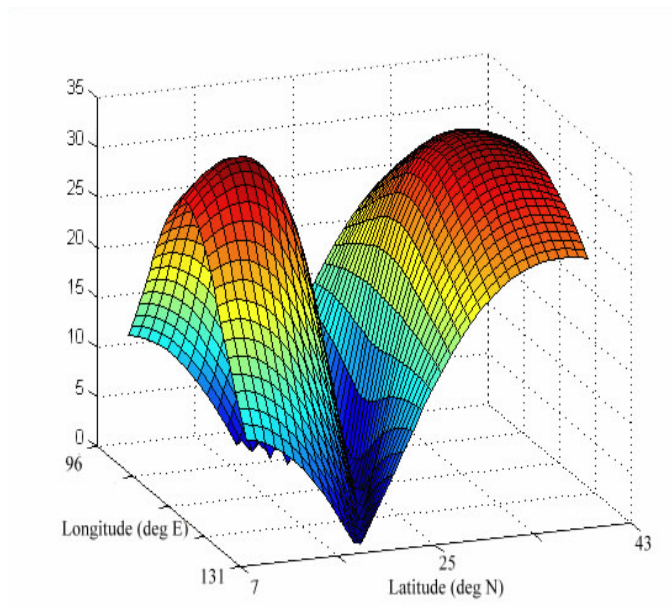


Fig. 17 Distribution of Φ_o in Sudan
 Φ_o in China.

Fig. 18 Distribution of

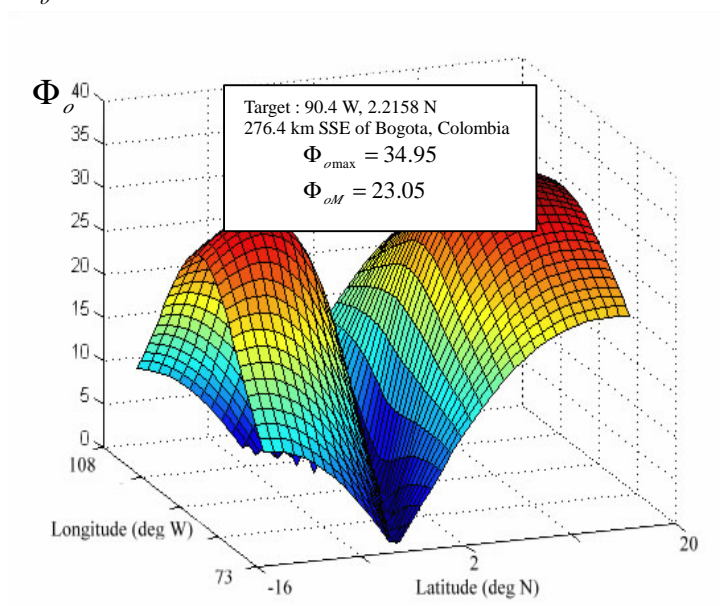


Fig. 19 Distribution of Φ_o in Colombia